Article

Structure

Characterization of an Additional Binding Surface on the p97 N-Terminal Domain Involved in Bipartite Cofactor Interactions

Graphical Abstract

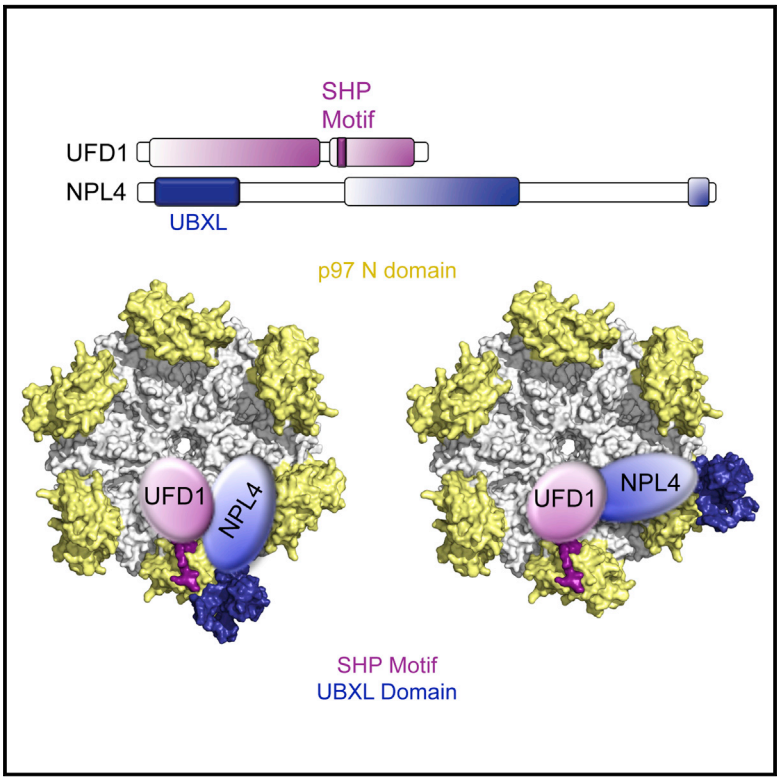

Authors

Petra Hänzelmann,
Hermann Schindelin

Correspondence

petra.haenzelmann@virchow.uni-wuerzburg.de

In Brief

The AAA ATPase p97 interacts with a large number of cofactors that regulate its function. Hänzelmann and Schindelin determined the structure of p97 in complex with a linear SHP peptide, which explains how cofactors can utilize a bipartite binding mechanism to interact with p97.

Highlights

- The SHP motif binds to a different site than other p97 N domain interacting cofactors
- The SHP-binding mode is conserved between structurally unrelated proteins
- The UFD1/NPL4 cofactor engages in a bipartite binding mode with the N domain
- Bipartite binding involves either a single or two adjacent N domains

Accession Numbers

5C1B

Hänzelmann & Schindelin, 2016, Structure *24*, 140–147
January 5, 2016
http://dx.doi.org/10.1016/j.str.2015.10.027

CellPress

Structure
Article

Characterization of an Additional Binding Surface on the p97 N-Terminal Domain Involved in Bipartite Cofactor Interactions

Petra Hänzelmann[1,*] and Hermann Schindelin[1]
[1]Rudolf Virchow Center for Experimental Biomedicine, University of Würzburg, Josef-Schneider-Straße 2, 97080 Würzburg, Germany
*Correspondence: petra.haenzelmann@virchow.uni-wuerzburg.de
http://dx.doi.org/10.1016/j.str.2015.10.027

SUMMARY

The type II AAA ATPase p97 interacts with a large number of cofactors that regulate its function by recruiting it to different cellular pathways. Most of the cofactors interact with the N-terminal (N) domain of p97, either via ubiquitin-like domains or short linear binding motifs. While some linear binding motifs form α helices, another group features short stretches of unstructured hydrophobic sequences as found in the so-called SHP (BS1, binding segment 1) motif. Here we present the crystal structure of a SHP-binding motif in complex with p97, which reveals a so far uncharacterized binding site on the p97 N domain that is different from the conserved binding surface of all other known p97 cofactors. This finding explains how cofactors like UFD1/NPL4 and p47 can utilize a bipartite binding mechanism to interact simultaneously with the same p97 monomer via their ubiquitin-like domain and SHP motif.

INTRODUCTION

p97 is a type II AAA ATPase (ATPase associated with a variety of cellular activities) (Ogura and Wilkinson, 2001; Wendler et al., 2012) with many roles in diverse biological functions, including ER-associated protein degradation (ERAD) and the ubiquitin proteasome system, but also fulfilling non-proteolytic functions (reviewed in Meyer et al., 2012; Meyer and Weihl, 2014; Stolz et al., 2011). This functional diversity is mediated with the help of a large variety of cofactors (reviewed in Yeung et al., 2008). p97 forms a hexamer with two stacked rings formed by the two ATPase domains (D1 and D2) with an N-terminal (N) domain attached to the D1 ring (Davies et al., 2008; Huyton et al., 2003). Cofactors either bind to the unstructured C terminus or the N domain. Due to its involvement in several important cellular processes, defects in interactions between p97 and its binding partners contribute to various diseases, while p97 itself has been linked to cancer and a wide variety of neurodegenerative disorders (reviewed in Meyer and Weihl, 2014). Mutations in p97 are causative of two fatal protein aggregation diseases (proteinopathies): inclusion body myopathy with Paget's disease of the bone and frontotemporal dementia (IBMPFD) and familial amyotrophic lateral sclerosis (fALS) (Meyer and Weihl, 2014).

Currently known cofactors interact with the N domain via either a ubiquitin regulatory X (UBX) domain and other domains with a ubiquitin-like fold (UBX-like, UBXL) or through one of several linear binding motifs (Morreale et al., 2009; Yeung et al., 2008). The latter include the VCP-interacting motif (VIM), the VCP-binding motif (VBM), and the SHP motif (also known as binding site 1 [BS1]). The VIM and VBM motifs are short Arg/Lys-rich peptide stretches that bind as α helices to p97 (Hänzelmann and Schindelin, 2011; Liu et al., 2013a), whereas the SHP-binding motif is a short sequence stretch enriched in hydrophobic amino acids. Although there is no sequence similarity between the VIM-binding motif (Hänzelmann and Schindelin, 2011) and the UBX domain (e.g., Dreveny et al., 2004; Hänzelmann et al., 2011) or UBXL domains (Isaacson et al., 2007; Kim et al., 2014), the binding sites partly overlap and all cofactors bind to the same general area centered on the hydrophobic interdomain cleft between the two subdomains of p97 N, thus explaining why these cofactors compete with each other (Ballar et al., 2006; Bruderer et al., 2004; Hänzelmann and Schindelin, 2011; Meyer et al., 2000; Nagahama et al., 2003).

There are two major cofactors of p97, the UFD1/NPL4 complex and p47, which form independent complexes with p97. UFD1 and NPL4 form a heterodimer (Meyer et al., 2000; Pye et al., 2007): UFD1 comprises (Figure 1A) an N-terminal domain (UT3), which is structurally similar to the N domain of p97 and contains binding sites for both poly- and mono-ubiquitin (Park et al., 2005; Rumpf and Jentsch, 2006), and a C-terminal domain (UT6) involved in NPL4 binding also harboring a SHP-binding motif (SHP1) for p97 interaction (Bruderer et al., 2004). NPL4 is composed of an N-terminal UBXL domain that interacts with p97 (Bruderer et al., 2004; Isaacson et al., 2007), a C-terminal zinc finger domain (NZF) domain that binds ubiquitin (Wang et al., 2003), and a centrally located catalytically inactive MPN domain of unknown function (Figure 1A). The interaction between the heterodimeric UFD1/NPL4 and p97 is bipartite as it is mediated through the SHP1 motif in UFD1 and the UBXL domain of NPL4 (Bruderer et al., 2004). It has been proposed that these sites interact with two different N domains (Isaacson et al., 2007). p47 contains three domains connected by long flexible regions (Figure 1A): an N-terminal UBA (ubiquitin-associated) domain involved in ubiquitin interaction, a central SEP domain, which is involved in trimerization, and a C-terminal UBX domain that interacts with p97 (Beuron et al., 2006; Dreveny et al., 2004). The flexible linker connecting the SEP and UBX

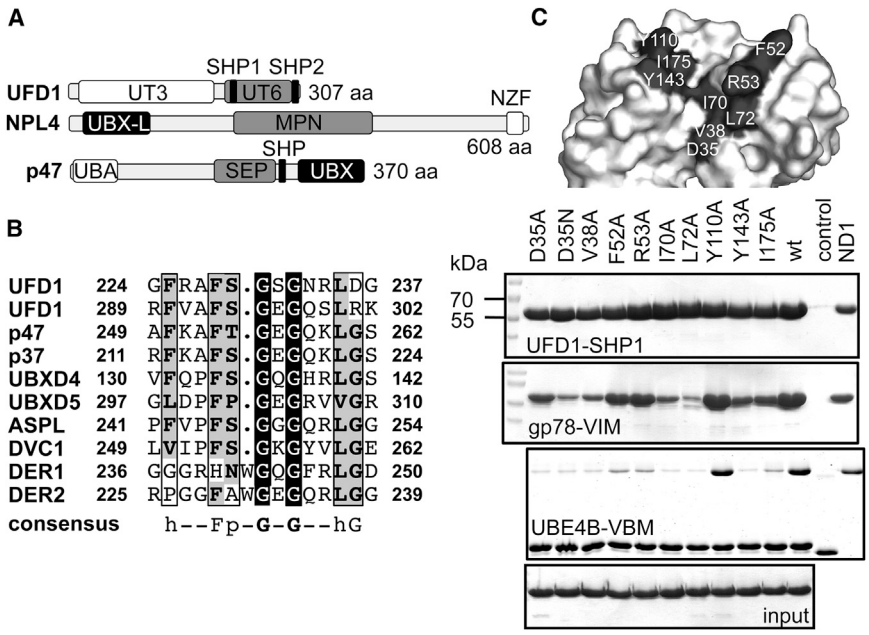

Figure 1. The SHP-Binding Motif

(A) Domain architectures of heterodimeric UFD1/NPL4 and p47.

(B) Sequence alignment of SHP-binding motifs currently identified in human proteins. Strictly conserved residues are highlighted with a black background and similar residues with a gray background.

(C) Top, surface representation of the p97N hydrophobic interdomain cleft, with residues important for UBX, VIM, and VBM cofactor interactions labeled. Bottom, streptavidin pull-down assays involving biotinylated peptides (UFD1-SHP1 and gp78-VIM) or GST pull-down assay (UBE4B-VBM) with p97ND1 wt and variants.

domains harbors a SHP motif. Like UFD1/NPL4, p47 also uses a bipartite mechanism to associate with p97 (Bruderer et al., 2004) utilizing its SHP motif and UBX domain.

Currently there is only limited structural information available as to how the SHP motif interacts with the N domain of p97. The SHP-binding site on p97 has been controversial, and either an alternative binding site (Bruderer et al., 2004) or a partially overlapping binding site with the UBXL of NPL4 (Isaacson et al., 2007) has been suggested. The crystal structure of the p97ND1-p47-UBX/SHP complex revealed that the SHP motif forms a crystal lattice contact with the N domain of a different hexamer (Dreveny et al., 2004). The observed binding site, which is different from the hydrophobic interdomain cleft of the N domain, was in agreement with an alternative binding site yet it was not characterized.

Here we present the crystal structure of p97 in complex with a SHP-binding motif, namely a peptide derived from UFD1, which revealed a so far uncharacterized interaction site on the N domain that is different from the binding surface of other p97 cofactors. The association of the SHP-binding motif on the lateral surface of the N domain and of UBX/UBXL domains in the hydrophobic interdomain cleft on top of the N domain allows for a bipartite binding of both binding domains/motifs to either the same N domain or to two adjacent N domains. This bipartite interaction mode not only increases the affinity but also restricts the conformational flexibility of p97.

RESULTS

Does the SHP-Binding Motif Target the Hydrophobic p97 N Interdomain Cleft?

The SHP-binding sequence which was first identified in Shp1, the yeast ortholog of p47, and in Dfm1p (Sato and Hampton, 2006), the yeast derlin 1 protein, was mapped to a short hydrophobic sequence stretch containing two invariant Gly residues and is typically characterized (Figure 1B) by the consensus sequence FxGxGx$_2$h (x, any amino acid; h, hydrophobic amino acid). The binding sequence is highly variable and typically found in an unstructured region of the protein. In mammals, this motif is found in the SEP domain containing UBX proteins p37, p47, UBXD4, and UBXD5 and in the UBX protein ASPL (Kloppsteck et al., 2012). The SHP motif is located N-terminally of the UBX domain, to which it is connected via a mainly unstructured linker. Additional SHP-binding motif-containing proteins are UFD1 (Bruderer et al., 2004), DVC1 (Spartan) (Mosbech et al., 2012), which functions in DNA repair coupled to DNA replication, and the DERLIN proteins (DER1 and DER2), which are involved in ERAD (Greenblatt et al., 2011; Huang et al., 2013). In UFD1, a second SHP motif (SHP2) was identified located at its extreme C terminus, which, however, seems not to be involved in interactions with p97 (Bruderer et al., 2004).

Initial streptavidin pull-down assays using a biotinylated UFD1 peptide covering the SHP1 motif revealed a strong binding to full-length p97 and the ND1 fragment (Figure 1C), whereas only a very weak interaction with the isolated N domain could be detected (data not shown), thus suggesting that further structural elements like the linker between the N and D1 domain and/or the D1 domain are required. To further characterize this interaction, we analyzed ND1 variants (Figure 1C) of the N domain hydrophobic interdomain cleft, which harbors the binding region for UBX and VIM proteins (Hänzelmann et al., 2011; Hänzelmann and Schindelin, 2011). However, the streptavidin pull-down assay did not show a significant effect with any of the tested variants. These data suggest that the SHP motif utilizes a different and so far uncharacterized binding site. In contrast, the VIM of gp78 and the GST-tagged VBM of UBE4B, which is involved in multi-ubiquitin chain assembly (Laser et al., 2006), revealed a largely impaired interaction with most of the residues, confirming the proposed binding site of the VBM on the N domain (Liu et al., 2013a) as being similar to the VIM-binding region.

The Structural Basis for p97-SHP Binding

To elucidate the molecular basis of SHP recognition by p97, we determined the crystal structure of full-length p97 in complex with a UFD1-derived peptide encompassing the SHP1 motif. The 3.1-Å structure was solved by molecular replacement and

Table 1. Data Collection and Refinement Statistics

Data Collection	
Wavelength (Å)	0.97625
Resolution (Å)	49.14–3.08 (3.13–3.08)
Space group	$P2_12_12_1$
Cell dimensions	
a, *b*, *c* (Å)	140.7, 180.7, 255.0
Unique reflections	120,596
$<I/\sigma(I)>$	12.8 (1.1)
Completeness (%)	100 (99.9)
Redundancy	11.0 (10.9)
R_{sym}	0.116 (2.495)
R_{pim}	0.053 (1.155)
CC (1/2)	0.999 (0.527)
Refinement	
Resolution limits (Å)	49.14–3.08
Number of reflections	120,478
R_{cryst}/R_{free}	0.198 (0.240)
Number of atoms	
Protein (non-hydrogen)	34,227
Ligands	402
Solvent atoms	30
Root mean square deviations in	
Bond lengths (Å)	0.003
Bond angles (°)	0.730
Coordinate error (Å)	0.40
Average B factors (Å^2)	
Overall	146
N (chain D)[a]	184
D1 (chain D)[a]	136
D2 (chain D)[a]	140
UFD1 peptide (chain V)[a]	220
Ramachandran Statistics (%)	
Favored	96.21
Allowed	3.10
Outliers	0.69

[a]B factors are for the p97-UFD1 peptide complex found in chains D and V.Statistics for the highest-resolution shell are shown in parentheses.

was refined to R_{free} and R values of 24.0% and 19.8%, respectively (Table 1). A region of unassigned electron density in two of the six N domains was found in both the $2F_o - F_c$ and $F_o - F_c$ electron density maps (Figure 2A). Eleven residues (amino acids [aa] 225–235) of the 21-amino acid peptide were defined and could be modeled (Figure 2A). The peptide adopts a mostly extended conformation and is attached on the outside of the C-terminal $\alpha + \beta$ subdomain (Nc, aa 112–186) of the N domain in a region that is directly adjacent to the ND1 linker (Figure 2B). The peptide associates with two β strands of the four-stranded β sheet, and is further stabilized by an α helix. Although the N domains in this structure are rather flexible, and many side chains are disordered, which are further translated to the bound peptide (average B factors for all atoms: N, 184 Å^2; D1, 136 Å^2; D2, 140 Å^2; UFD1 peptide, 220 Å^2), it was possible to assign the N-terminal part of the peptide including the two Phe residues. However, in the region of the invariant GxG motif, the electron density is less well defined and the side chain orientation of the following C-terminal part is not entirely clear. Participating residues from p97 include R113, H115, F131, and H183, and in UFD1, residues F225, F228, and R234 are involved (Figure 2C). The interaction is mainly hydrophobic in nature, and only a few electrostatic contacts are observed. UFD1 F225 is involved in hydrophobic interactions with L117 of p97, while p97 R113 and UFD1 R234 engage in hydrophobic contacts via their long aliphatic side chains with UFD1 F228 and p97 F131, respectively. The side chains of the p97 H115 and H183 are in hydrogen-bonding distance to the main-chain atoms of A227, S229, and S231 in UFD1.

Analysis of the p97-SHP Interface

A mutational analysis was carried out to determine the functional significance of the molecular interactions observed in the complex. Streptavidin pull-down assays revealed that R113, H115, F131, and H183 of p97 are important, with the single F131A and H183A variants already completely abolishing the interaction (Figure 2D). E185 largely retained the ability to interact with p97, and V181 was found not to be involved. For the UFD1-SHP1 motif peptide, these studies revealed that F225, F228, and R234 contributed significantly to binding, whereas N233 and L235 only played a minor role (Figure 2E). These data clearly validated the binding mode observed in the crystal structure.

To confirm that the data obtained with the peptide also apply to the full-length protein an isothermal titration calorimetry (ITC) analysis of the heterodimeric UFD1/NPL4 complex with the p97ND1 fragment was carried out (Figures 3 and S1). The p97 Ala variants of R113, H115, F131, and H183 showed a largely reduced interaction (7- to 16-fold decrease in the dissociation constant K_D) compared with the wild type (wt), whereas the E185A substitution did not alter the affinity (Figures 3B and S1). The same applied to the UFD1 variants as already single Ala substitutions of F225, F228, and R234 showed an impaired interaction, with a 5- to 8-fold decrease in K_D (Figures 3C and S1). As mentioned earlier, UFD1 contains, at its extreme C terminus, 65 amino acids downstream of the verified SHP motif (SHP1), a closely related second SHP (SHP2) sequence (Figure S2A) located in an unstructured region, which, theoretically, could associate with an additional N domain and thereby provide even more specificity. However, based on a GST pull-down analysis of a short fragment comprising the last 26 residues of UFD1, no interaction with p97 was detected (Bruderer et al., 2004), which may be explained by the exchange of the important SHP1 R234 with a Ser (Figure S2A). Nevertheless, an ITC analysis using the heterodimeric UFD1/NPL4 complex in which the last 21 amino acids of UFD1 were missing (ΔSHP2), revealed a 3-fold decrease in affinity (Figures S2B and S2C), suggesting a weak contribution of SHP2 to the binding affinity. However, since single SHP1 mutants displayed an even more severe effect (Figure 3C), it cannot be ruled out that structural changes are the reason for the weaker affinity. Interestingly, a UFD1 mutant, where both binding motifs were swapped, still showed an affinity comparable with the wt protein (Figures S2B and S2C), indicating that the SHP2 motif is functional if it is located in the proper position. These data point toward an interplay between

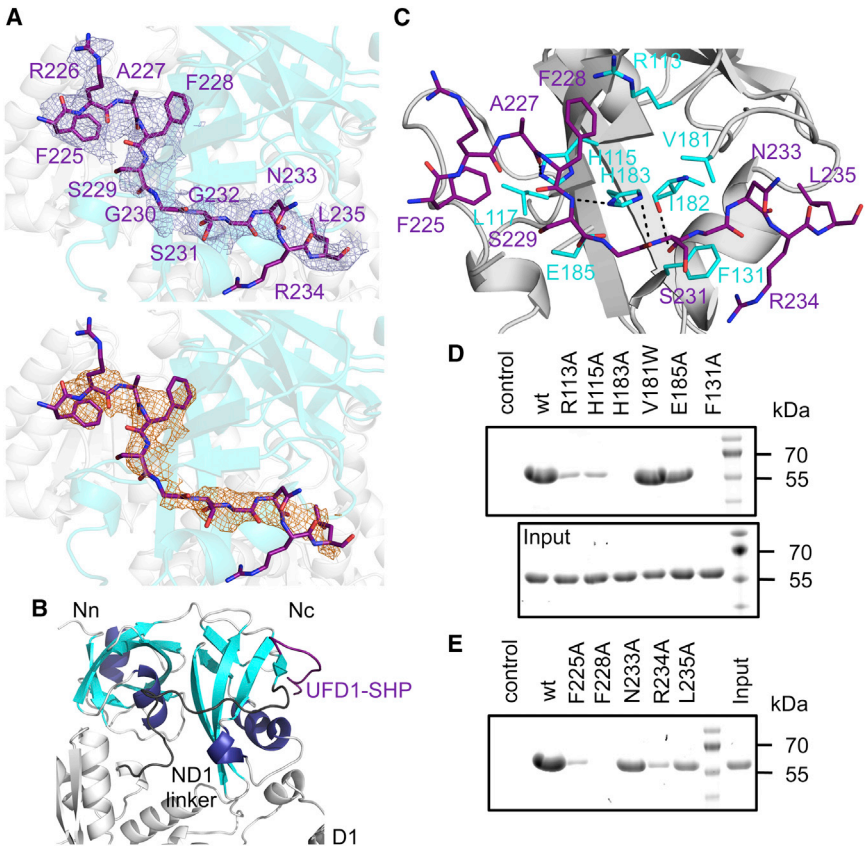

Figure 2. Structure of p97 in Complex with the UFD1-SHP1-Binding Motif

(A) Top, SIGMAA-weighted $2F_o - F_c$ electron density map of the UFD1 peptide shown in stick representation (colored according to atom type with C atoms in purple) contoured at 0.9 times the root mean square deviation (RMSD), with a cartoon representation of the N domain in cyan and the D1 domain in gray. Bottom, Unbiased SIGMAA-weighted $F_o - F_c$ electron density map contoured at 2.8 times the RMSD.

(B) Cartoon representation of p97 in complex with the UFD1 peptide (Nn and Nc subdomains are shown with β strands in cyan and α helices in blue, D1 in gray, ND1 linker in black, UFD1 peptide in purple, D2 not shown).

(C) Cartoon representation of the binding interface. Residues involved in binding are shown in stick representation, with the UFD1 peptide colored in purple and p97N residues in cyan. Dashed lines indicate putative H bonds.

(D) Streptavidin pull-down assays of biotinylated UFD1-SHP1 wt peptide with p97ND1 (wt and variants).

(E) Streptavidin pull-down assays of p97ND1 wt with biotinylated UFD1-SHP1 peptides (wt and variants).

both SHP motifs, which may be even more pronounced when additional cofactors are present. Whether both motifs can also be used in vivo remains to be elucidated.

To further investigate the functional significance of the SHP motif and to find out whether the observed binding mode also applies to other SHP motif-containing proteins, we analyzed the UBX protein p47, since it contains the SHP motif and UBX domain on the same polypeptide separated only by a linker. Interestingly, an earlier crystal structure of the ND1 fragment of p97 in complex with the C-terminal region of p47, composed of its UBX domain and SHP motif (Dreveny et al., 2004), revealed that the SHP motif forms a lattice contact with the Nc domain from a different hexamer instead of associating with its own N domain (Figure 3D). Nevertheless, the binding region involving H115, F131, and H183 is identical to the identified UFD1-SHP-binding site (Figure 3E), and the flexible linker connecting the UBX domain and the SHP-binding motif would be of sufficient length to also allow the association of the SHP motif with the same N domain to which UBX is bound (Figure 3D). Since the interaction site present in this structure was not further characterized, we conducted ITC analyses of wt p47 and ND1 variants. These studies yielded similar results as for UFD1/NPL4, with the F131A and H183A variants displaying the largest reduction in binding, thus indicating a conserved interaction mode (Figures 3F and S3A) with the exception of the H115A variant, which showed only a slight decrease (2-fold) in affinity. This difference could be due to the different binding modes involving either two proteins in the case of the UFD1/NPL4 heterodimer, or just one protein for p47, which, in the latter case, may restrict the way in which the SHP motif interacts with its binding surface.

The structure of the NPL4-UBXL domain was solved by nuclear magnetic resonance and, based on chemical shift experiments, a structural model for the p97N–NPL4-UBXL complex was calculated (Isaacson et al., 2007). Based on this model, R8 as well as F76 make significant contributions to p97N binding (Figure 3A). We introduced Ala residues at both positions to elucidate the contribution of NPL4 binding to p97. While the UFD1/NPL4-F76A variant could not be purified in sufficient amounts, indicating that the removal of the bulky hydrophobic side chain affects protein stability, the UFD1/NPL4-R8A variant significantly impaired the interaction to a similar extent as observed for the UFD1 variants in ITC experiments (Figures 3C and S1). In addition, analysis of the two N domain variants (Figures 3B and S1), D55A and Y110A, residues that are involved in interactions with the UBXL of NPL4 (Figure 3A), and hence should not interfere with binding of the SHP motif, almost completely abolished this interaction (40- to 50-fold decrease in K_D). In contrast, based on the structure of the p47-UBX domain bound to p97ND1 (Dreveny et al., 2004), D55 is not involved in the interaction with this UBX domain, and Y110 only makes a minor contribution. Accordingly, ITC analysis revealed wt affinity for the D55A variant and only a 2-fold decrease in the affinity for the Y110A variant (Figure S3B), which further demonstrated that D55 and Y110 were not involved in SHP binding, and that the binding defect with UFD1/NPL4 was the consequence of an abolished NPL4 interaction. Earlier studies proposed that the NPL4-UBXL is the general p97-binding domain and that binding of UFD1 provides higher affinity and positions the cofactor in the correct orientation with respect to p97 for interaction with ubiquitylated

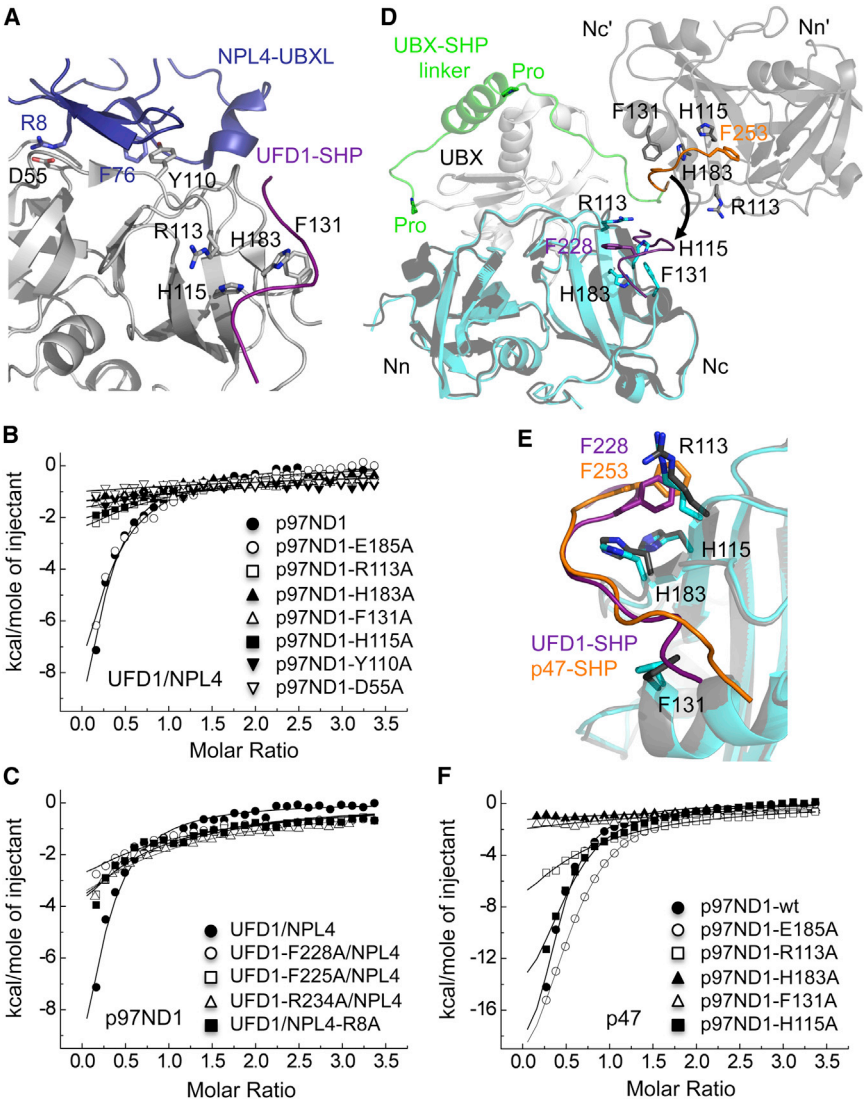

Figure 3. Interaction of p97 with UFD1/NPL4 and p47

(A) Cartoon representation of p97N (colored in gray) in complex with the NPL4-UBXL domain (PDB: 2PJH; Isaacson et al., 2007, colored in blue) and the UFD1-SHP1-binding motif (colored in purple) as a model for bipartite binding to the same N domain. Residues involved in binding are shown in stick representation colored according to atom type.

(B) ITC analysis of p97ND1 (wt and variants) with UFD1/NPL4 wt. See also Figure S1.

(C) ITC analysis of p97ND1 wt with UFD1/NPL4 (wt and variants). See also Figures S1 and S2.

(D) Superposition of the p97N–UFD1-SHP1 (N colored in cyan, UFD1-SHP colored in purple) and p97N–p47-UBX/SHP complexes (PDB: 1S3S (Dreveny et al., 2004), with the N domain in dark gray, symmetry-related N domain in medium gray, UBX in light gray, p47-SHP in orange, UBX-SHP linker in green). Residues involved in binding are shown in stick representation colored according to atom type. The arrow relates the SHP peptides.

(E) Superposition of the UFD1 (p97N colored in cyan, SHP colored in purple) and p47 (1S3S; Dreveny et al., 2004, p97N colored in gray, SHP colored in orange) SHP-binding motifs.

(F) ITC analysis of p97ND1 (wt and variants) with p47 wt. See also Figure S3A.

substrates (Bruderer et al., 2004). However, our data clearly show that a bipartite binding mode involving both the UBXL and SHP is essential for the interaction with p97, with the UBXL domain apparently making a stronger contribution. Already single variants either affecting UBXL/UBX or SHP binding largely impaired the interaction of p97 with its UFD1/NPL4 and p47 cofactors.

DISCUSSION

The data presented here characterize in detail a binding surface on the N domain, which associates with the SHP motifs of UFD1 and p47. This site is different from the common binding site of UBX and UBXL domains, as well as the α-helical VIM- and VBM-binding motifs, which all interact with the hydrophobic interdomain cleft formed between the two subdomains of the N domain (Figure 4A). Unlike the UBX domain and the VIM-binding motif, the SHP motif does not recognize an isolated N domain (aa 1–187). This can be explained by the fact that the binding surface on the N domain includes residues from the last β strand that precedes the ND1 linker, as well as E185, the first residue of the linker. Furthermore, a superposition of the N domain in complex with the SHP peptide and the isolated N domain revealed an altered conformation of aa 183–187, which would prevent SHP binding (Figure S4).

The crystal structure of the p97–p47-UBX/SHP complex together with the identification of the UFD1-SHP-binding site on the Nc subdomain, indicate that both binding domains/motifs may associate with the same N domain and do not bind to two adjacent N domains, at least for UBX proteins like p47 that contain both domains/motifs on the same polypeptide separated by a flexible linker (Figure 4B). In theory, this would allow additional cofactors to assemble with a p97 hexamer via unoccupied N domains (see later). This would be consistent with the earlier finding that both isolated binding motifs/domains can bind independently (Bruderer et al., 2004). However, it cannot be ruled out that the long flexible linker adopts a different conformation mediated by the embedded Pro residues (Figure 3D) and points in the opposite direction so that the SHP motif binds to an adjacent N domain. Both models would be consistent with electron microscopy (EM) studies of the p97–p47 complex in different nucleotide states (Beuron et al., 2006), suggesting that, during ATP hydrolysis, binding of trimeric p47 via its UBX domains either involves only every second N domain or all six N domains where the UBX domain and its upstream linker are bound between two adjacent N domains (Figure 4B).

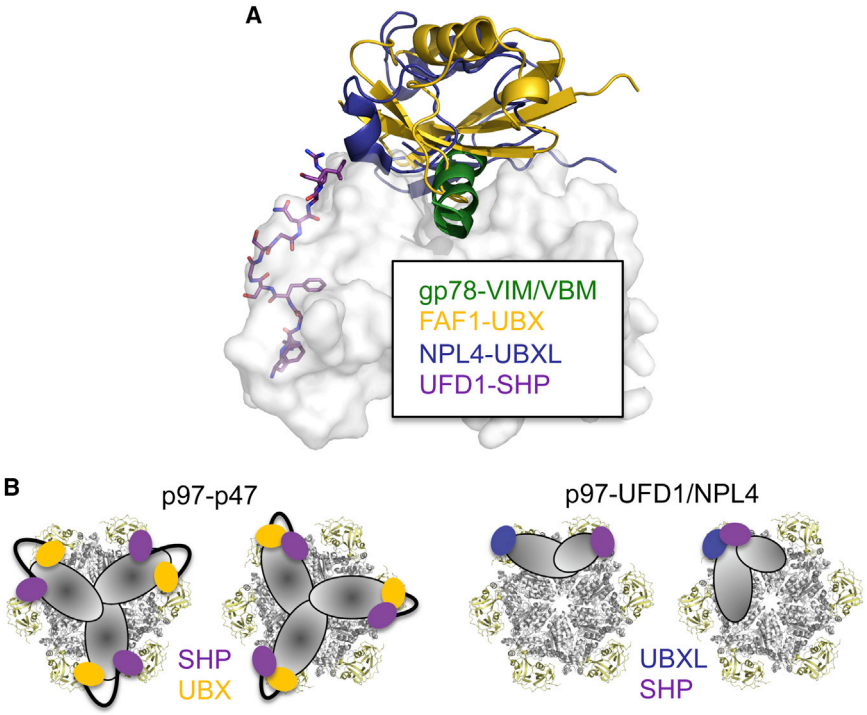

Figure 4. Cofactor Binding to the p97 N Domain

(A) Ribbon representations together with the molecular surface of p97N in complex with the VIM of gp78 (PDB: 3TIW; Hänzelmann and Schindelin, 2011, colored in green), FAF1-UBX (PDB: 3QQ8; Hänzelmann et al., 2011, colored in gold) and NPL4-UBXL (PDB: 2PJH; Isaacson et al., 2007, colored in blue). The UFD1-SHP1 peptide (colored according to atom type with C-atoms in purple) is shown in stick representation. See also Figure S4.

(B) Models for the interaction of p97, with either p47 (left two panels) or UFD1/NPL4 (right two panels) involving bipartite binding to either different (left in each case) or identical (right in each case) N domains.

In the case of UFD1/NPL4, where the binding domains/motifs reside on separate proteins, the mode of bipartite binding is still undefined. Although it has been proposed that the NPL4-UBXL domain and the UFD1-SHP-binding sites are on adjacent N domains (Isaacson et al., 2007), and despite the existence of EM structures depicting the p97–UFD1/NPL4 complex (Bebeacua et al., 2012; Pye et al., 2007), there is currently no direct evidence for this model (Figure 4B). Earlier studies showed that chemical shift perturbations induced in spectra of p97 N in the presence of an UFD1-SHP1 peptide are reversed upon the addition of the NPL4-UBXL domain, which suggests a degree of communication between the NPL4- and UFD1-binding sites on p97 (Isaacson et al., 2007). These data would be in agreement with the crystal structure of p97 in complex with the UFD1-SHP1 motif and the structural model for the p97N–NPL4-UBXL complex (Isaacson et al., 2007). The last ordered residues of the peptide are in close proximity to the UBXL, and the C terminus of the UBXL points toward the peptide (Figure 4A), suggesting some degree of steric hindrance between the full-length proteins, thus favoring a model with binding sites on two adjacent N domains (Figure 4B). In contrast, based on the work with peptides of the UFD1 and p47 SHP motifs, and the isolated NPL4-UBXL and p47-UBX domain, it could be shown in pull-down experiments that both binding motifs/domains bind independently (Bruderer et al., 2004), indicating binding to the same N domain. Thus, none of the proposed models can be ruled out at this time (Figure 4B).

Whether cofactors always stay associated via both binding motifs is not known. It is conceivable that, for example, during ATP hydrolysis or substrate-binding, conformational changes are induced that lead to the dissociation of one site, thus weakening the interaction and resulting in an increased conformational flexibility of the cofactor for subsequent catalysis. Such a model would be in accordance with the conformational variability observed in the EM structures of the p97–UFD1/NPL4 complex in different nucleotide state where the heterodimer is bound either via two or just a single binding site (Bebeacua et al., 2012) and the EM studies of the p97–p47 complex as described above (Beuron et al., 2006). Irrespective of the question whether the same or different N domains are targeted, due to avidity effects, a bipartite binding generally enhances the affinity of individually weaker interactions and allows for greater binding specificity.

Structural studies of IBMPFD-associated p97 mutants revealed dramatic nucleotide-dependent conformational changes in the position of the N domain (Tang et al., 2010), and an altered interaction with cofactors has been shown in vivo (Fernandez-Saiz and Buchberger, 2010). In particular, increased amounts of UFD1/NPL4 and p47 were found in cells. The movement of the N domains from a position in a plane with the D1 domain to a position above the D1 domain could bring the cofactors into close spatial proximity, leading to a tighter binding on top of p97 assisted by an enhanced bipartite binding mode.

One of the key questions regarding the biological function of p97 is how this highly abundant ATPase participates in so many dissimilar processes? This functional diversity is mainly the result of its association with a large variety of cofactors, which is regulated by multiple mechanisms (reviewed in Buchberger et al., 2015). The heterodimeric UFD1/NPL4 and trimeric p47 cofactors form p97 complexes differ significantly in stoichiometry and symmetry, providing the structural basis for the mutually exclusive binding of p47 and UFD1/NPL4 to p97 (Bruderer et al., 2004; Meyer et al., 2000). Since only one heterodimeric UFD1/NPL4 cofactor binds to the p97 hexamer, further cofactors could potentially bind to vacant N domains. Indeed, it was shown that immunoprecipitates of the UBA-UBX proteins FAF1, UBXD7, UBXD8, and SAKS1 contained not only p97, but also UFD1/NPL4 (Alexandru et al., 2008), an observation that is consistent with the existence of higher-order p97-cofactor complexes. In addition to the UBA-UBX proteins discussed earlier, the UFD1/NPL4 heterodimer was also found in quaternary complexes with p97 and the deubiquitinating (DUB) enzyme

Otu1/YOD1 (Ernst et al., 2009; Kim et al., 2014), the VBM cofactor NUB1L (Liu et al., 2013b), and the VIM protein SelS/VIMP (Ye et al., 2004). In addition, for p47, it was proposed that the DUB VCIP135 forms, via its UBXL domain, an unstable ternary complex, where p47 would be associated via only one of its binding sites (Uchiyama et al., 2002).

In summary, our structural and functional characterization of the bipartite binding mode of UFD1/NPL4 and p47 provides crucial insights into p97 cofactor specificity/diversity, and the assembly of higher-order p97-cofactor complexes, which is tightly controlled by multiple regulatory mechanisms including mutually exclusive binding, different oligomeric assemblies, and nucleotide-dependent conformational changes.

EXPERIMENTAL PROCEDURES

Cloning, Site-Directed Mutagenesis, Protein Expression, and Purification

The following constructs were used in this study: human full-length p97 (aa 1–806), p97N (aa 1–187), p97ND1 (aa 1–480), human UFD1 and NPL4, human p47 (Hänzelmann et al., 2011; Hänzelmann and Schindelin, 2011); human GST-tagged UBE4B-VBM (aa 1–23, pETM30, EMBL Heidelberg, NcoI/XhoI). p97Δ709-728 was generated by PCR mutagenesis. For site-directed mutagenesis, the QuikChange II Site-Directed Mutagenesis Kit from Agilent was used. Unmodified as well as N-terminally biotinylated (Biotin-Ahx) human peptides were purchased from Genscript: UFD1 (^{221}GELGFRAFSGSGNRLDGKKKG^{241}), gp78 (^{622}VTLRRRMLAAAAERRLQKQ^{640}). Protein expression and purification was performed as described using metal-affinity and size-exclusion chromatography (Hänzelmann et al., 2011; Hänzelmann and Schindelin, 2011). The purification protocol of p97Δ709-728 included an additional anion-exchange chromatography step (Q-sepharose FF, GE Healthcare) using a 100 mM HEPES (pH 7), 50 mM NaCl, and 5 mM β-mercatoethanol buffer, and a linear NaCl gradient (0.05–500 mM).

Crystallization

For crystallization of p97Δ709-728 in complex with the UFD1 peptide, p97Δ709-728 was incubated with ATPγS and the peptide at a molar ratio of 1:15:5 (0.1 mM p97, 1.5 mM ATPγS, and 0.5 mM peptide) for 1 hr at 4°C. Crystals were grown at 20°C by vapor diffusion in hanging drops containing equal volumes of protein in 10 mM HEPES (pH 8), 100 mM NaCl, 5 mM $MgCl_2$, and 1 mM TCEP, and a reservoir solution consisting of 6.5%–7% (w/v) polyethylene glycol 4000, 0.4–0.6 M potassium acetate, and 100 mM MES (pH 5.75).

Data Collection and Structure Determination

Crystals were cryo-protected by soaking in mother liquor containing increasing concentrations (5%–30%, v/v) of glycerol, flash cooled in liquid nitrogen, and data collection was performed at 100 K. Data were collected at beamline ID29 (ESRF) and processed using XDS (Kabsch, 2010). For subsequent calculations, the CCP4 suite (Winn et al., 2011) and Phenix (Adams et al., 2010) were utilized. Phases were obtained by molecular replacement using Phaser (McCoy et al., 2007) searching for two trimers (PDB: 3CF3; Davies et al., 2008). The structure was refined with Phenix incorporating non-crystallographic symmetry restraints and TLS refinement in all cycles.

In Vitro Binding Assays

ITC experiments were conducted as described (Hänzelmann et al., 2011), using 50 mM Tris (pH 8), 150 mM KCl, and 5 mM $MgCl_2$ as buffer. In all experiments, a 15-fold molar excess of UFD1/NPL4 or p47 was titrated into the sample cell containing 10 μM p97ND1. A volume of 10 μl of ligand was added at a time, with a total of 30 injections. All experiments were performed using a VP-ITC instrument (MicroCal, GE Healthcare) at 25°C. Data were analyzed with a single-site binding model using the software supplied by the ITC manufacturer and nonlinear least-squares fitting to calculate the K_D. Pull-down assays using biotinylated or GST-tagged peptides were performed as previously described (Hänzelmann and Schindelin, 2011). Biotinylated peptides or GST-tagged proteins were immobilized on Strep-Tactin Sepharose beads (IBA BioTAGnology) or glutathione Sepharose beads (GSH, Novagen). In all experiments, 10 μl of beads were incubated with 12.5 μM biotinylated peptides/1 μM GST-tagged proteins in 200 μl of PBS buffer (pH 7.4) with 0.1% (v/v) Triton X-100 at 4°C for 1 hr. p97ND1 alone was included as control. After centrifugation (1,250 × *g*, 30 s) beads were washed four times with 400 μl of binding buffer. Equimolar amounts of purified p97ND1 and variants in a total volume of 200 μl of binding buffer were added to immobilized peptides, and treated in the same way as in the first step. Immobilized proteins were directly analyzed by 15% (v/v) SDS-PAGE.

ACCESSION NUMBERS

Atomic coordinates and structure factors have been deposited in the PDB with accession code PDB: 5C1B.

SUPPLEMENTAL INFORMATION

Supplemental Information includes four figures and can be found with this article online at http://dx.doi.org/10.1016/j.str.2015.10.027.

ACKNOWLEDGMENTS

This work was supported by the Deutsche Forschungsgemeinschaft (HA 3405/3-1 and the Rudolf Virchow Center for Experimental Biomedicine, FZ 82) to P.H. and H.S. We thank Dr. Antje Schäfer for critical reading of the manuscript.

Received: June 15, 2015
Revised: October 29, 2015
Accepted: October 30, 2015
Published: December 17, 2015

REFERENCES

Adams, P.D., Afonine, P.V., Bunkoczi, G., Chen, V.B., Davis, I.W., Echols, N., Headd, J.J., Hung, L.W., Kapral, G.J., Grosse-Kunstleve, R.W., et al. (2010). PHENIX: a comprehensive Python-based system for macromolecular structure solution. Acta Crystallogr. D Biol. Crystallogr. *66*, 213–221.

Alexandru, G., Graumann, J., Smith, G.T., Kolawa, N.J., Fang, R., and Deshaies, R.J. (2008). UBXD7 binds multiple ubiquitin ligases and implicates p97 in HIF1alpha turnover. Cell *134*, 804–816.

Ballar, P., Shen, Y., Yang, H., and Fang, S. (2006). The role of a novel p97/valosin-containing protein-interacting motif of gp78 in endoplasmic reticulum-associated degradation. J. Biol. Chem. *281*, 35359–35368.

Bebeacua, C., Forster, A., McKeown, C., Meyer, H.H., Zhang, X., and Freemont, P.S. (2012). Distinct conformations of the protein complex p97-Ufd1-Npl4 revealed by electron cryomicroscopy. Proc. Natl. Acad. Sci. USA *109*, 1098–1103.

Beuron, F., Dreveny, I., Yuan, X., Pye, V.E., McKeown, C., Briggs, L.C., Cliff, M.J., Kaneko, Y., Wallis, R., Isaacson, R.L., et al. (2006). Conformational changes in the AAA ATPase p97-p47 adaptor complex. EMBO J. *25*, 1967–1976.

Bruderer, R.M., Brasseur, C., and Meyer, H.H. (2004). The AAA ATPase p97/VCP interacts with its alternative co-factors, Ufd1-Npl4 and p47, through a common bipartite binding mechanism. J. Biol. Chem. *279*, 49609–49616.

Buchberger, A., Schindelin, H., and Hänzelmann, P. (2015). Control of p97 function by cofactor binding. FEBS Lett. *589*, 2578–2589.

Davies, J.M., Brunger, A.T., and Weis, W.I. (2008). Improved structures of full-length p97, an AAA ATPase: implications for mechanisms of nucleotide-dependent conformational change. Structure *16*, 715–726.

Dreveny, I., Kondo, H., Uchiyama, K., Shaw, A., Zhang, X., and Freemont, P.S. (2004). Structural basis of the interaction between the AAA ATPase p97/VCP and its adaptor protein p47. EMBO J. *23*, 1030–1039.

Ernst, R., Mueller, B., Ploegh, H.L., and Schlieker, C. (2009). The otubain YOD1 is a deubiquitinating enzyme that associates with p97 to facilitate protein dislocation from the ER. Mol. Cell *36*, 28–38.

Fernandez-Saiz, V., and Buchberger, A. (2010). Imbalances in p97 co-factor interactions in human proteinopathy. EMBO Rep. *11*, 479–485.

Greenblatt, E.J., Olzmann, J.A., and Kopito, R.R. (2011). Derlin-1 is a rhomboid pseudoprotease required for the dislocation of mutant alpha-1 antitrypsin from the endoplasmic reticulum. Nat. Struct. Mol. Biol. *18*, 1147–1152.

Hänzelmann, P., and Schindelin, H. (2011). The structural and functional basis of the p97/valosin-containing protein (VCP)-interacting motif (VIM): mutually exclusive binding of cofactors to the N-terminal domain of p97. J. Biol. Chem. *286*, 38679–38690.

Hänzelmann, P., Buchberger, A., and Schindelin, H. (2011). Hierarchical binding of cofactors to the AAA ATPase p97. Structure *19*, 833–843.

Huang, C.H., Hsiao, H.T., Chu, Y.R., Ye, Y., and Chen, X. (2013). Derlin2 protein facilitates HRD1-mediated retro-translocation of sonic hedgehog at the endoplasmic reticulum. J. Biol. Chem. *288*, 25330–25339.

Huyton, T., Pye, V.E., Briggs, L.C., Flynn, T.C., Beuron, F., Kondo, H., Ma, J., Zhang, X., and Freemont, P.S. (2003). The crystal structure of murine p97/VCP at 3.6 Å. J. Struct. Biol. *144*, 337–348.

Isaacson, R.L., Pye, V.E., Simpson, P., Meyer, H.H., Zhang, X., Freemont, P.S., and Matthews, S. (2007). Detailed structural insights into the p97-Npl4-Ufd1 interface. J. Biol. Chem. *282*, 21361–21369.

Kabsch, W. (2010). Xds. Acta Crystallogr. D Biol. Crystallogr. *66*, 125–132.

Kim, S.J., Cho, J., Song, E.J., Kim, H.M., Lee, K.E., Suh, S.W., and Kim, E.E. (2014). Structural basis for ovarian tumor domain-containing protein 1 (OTU1) binding to p97/valosin-containing protein (VCP). J. Biol. Chem. *289*, 12264–12274.

Kloppsteck, P., Ewens, C.A., Forster, A., Zhang, X., and Freemont, P.S. (2012). Regulation of p97 in the ubiquitin-proteasome system by the UBX protein-family. Biochim. Biophys. Acta *1823*, 125–129.

Laser, H., Conforti, L., Morreale, G., Mack, T.G., Heyer, M., Haley, J.E., Wishart, T.M., Beirowski, B., Walker, S.A., Haase, G., et al. (2006). The slow Wallerian degeneration protein, WldS, binds directly to VCP/p97 and partially redistributes it within the nucleus. Mol. Biol. Cell *17*, 1075–1084.

Liu, S., Fu, Q.S., Zhao, J., and Hu, H.Y. (2013a). Structural and mechanistic insights into the arginine/lysine-rich peptide motifs that interact with P97/VCP. Biochim. Biophys. Acta *1834*, 2672–2678.

Liu, S., Yang, H., Zhao, J., Zhang, Y.H., Song, A.X., and Hu, H.Y. (2013b). NEDD8 ultimate buster-1 long (NUB1L) protein promotes transfer of NEDD8 to proteasome for degradation through the P97UFD1/NPL4 complex. J. Biol. Chem. *288*, 31339–31349.

McCoy, A.J., Grosse-Kunstleve, R.W., Adams, P.D., Winn, M.D., Storoni, L.C., and Read, R.J. (2007). Phaser crystallographic software. J. Appl. Crystallogr. *40*, 658–674.

Meyer, H., and Weihl, C.C. (2014). The VCP/p97 system at a glance: connecting cellular function to disease pathogenesis. J. Cell. Sci. *127*, 3877–3883.

Meyer, H.H., Shorter, J.G., Seemann, J., Pappin, D., and Warren, G. (2000). A complex of mammalian ufd1 and npl4 links the AAA-ATPase, p97, to ubiquitin and nuclear transport pathways. EMBO J. *19*, 2181–2192.

Meyer, H., Bug, M., and Bremer, S. (2012). Emerging functions of the VCP/p97 AAA-ATPase in the ubiquitin system. Nat. Cell. Biol. *14*, 117–123.

Morreale, G., Conforti, L., Coadwell, J., Wilbrey, A.L., and Coleman, M.P. (2009). Evolutionary divergence of valosin-containing protein/cell division cycle protein 48 binding interactions among endoplasmic reticulum-associated degradation proteins. FEBS J. *276*, 1208–1220.

Mosbech, A., Gibbs-Seymour, I., Kagias, K., Thorslund, T., Beli, P., Povlsen, L., Nielsen, S.V., Smedegaard, S., Sedgwick, G., Lukas, C., et al. (2012). DVC1 (C1orf124) is a DNA damage-targeting p97 adaptor that promotes ubiquitin-dependent responses to replication blocks. Nat. Struct. Mol. Biol. *19*, 1084–1092.

Nagahama, M., Suzuki, M., Hamada, Y., Hatsuzawa, K., Tani, K., Yamamoto, A., and Tagaya, M. (2003). SVIP is a novel VCP/p97-interacting protein whose expression causes cell vacuolation. Mol. Biol. Cell *14*, 262–273.

Ogura, T., and Wilkinson, A.J. (2001). AAA+ superfamily ATPases: common structure–diverse function. Genes Cells *6*, 575–597.

Park, S., Isaacson, R., Kim, H.T., Silver, P.A., and Wagner, G. (2005). Ufd1 exhibits the AAA-ATPase fold with two distinct ubiquitin interaction sites. Structure *13*, 995–1005.

Pye, V.E., Beuron, F., Keetch, C.A., McKeown, C., Robinson, C.V., Meyer, H.H., Zhang, X., and Freemont, P.S. (2007). Structural insights into the p97-Ufd1-Npl4 complex. Proc. Natl. Acad. Sci. USA *104*, 467–472.

Rumpf, S., and Jentsch, S. (2006). Functional division of substrate processing cofactors of the ubiquitin-selective Cdc48 chaperone. Mol. Cell *21*, 261–269.

Sato, B.K., and Hampton, R.Y. (2006). Yeast Derlin Dfm1 interacts with Cdc48 and functions in ER homeostasis. Yeast *23*, 1053–1064.

Stolz, A., Hilt, W., Buchberger, A., and Wolf, D.H. (2011). Cdc48: a power machine in protein degradation. Trends Biochem. Sci. *36*, 515–523.

Tang, W.K., Li, D., Li, C.C., Esser, L., Dai, R., Guo, L., and Xia, D. (2010). A novel ATP-dependent conformation in p97 N-D1 fragment revealed by crystal structures of disease-related mutants. EMBO J. *29*, 2217–2229.

Uchiyama, K., Jokitalo, E., Kano, F., Murata, M., Zhang, X., Canas, B., Newman, R., Rabouille, C., Pappin, D., Freemont, P., et al. (2002). VCIP135, a novel essential factor for p97/p47-mediated membrane fusion, is required for Golgi and ER assembly in vivo. J. Cell. Biol. *159*, 855–866.

Wang, B., Alam, S.L., Meyer, H.H., Payne, M., Stemmler, T.L., Davis, D.R., and Sundquist, W.I. (2003). Structure and ubiquitin interactions of the conserved zinc finger domain of Npl4. J. Biol. Chem. *278*, 20225–20234.

Wendler, P., Ciniawsky, S., Kock, M., and Kube, S. (2012). Structure and function of the AAA+ nucleotide binding pocket. Biochim. Biophys. Acta *1823*, 2–14.

Winn, M.D., Ballard, C.C., Cowtan, K.D., Dodson, E.J., Emsley, P., Evans, P.R., Keegan, R.M., Krissinel, E.B., Leslie, A.G., McCoy, A., et al. (2011). Overview of the CCP4 suite and current developments. Acta Crystallogr. D Biol. Crystallogr. *67*, 235–242.

Ye, Y., Shibata, Y., Yun, C., Ron, D., and Rapoport, T.A. (2004). A membrane protein complex mediates retro-translocation from the ER lumen into the cytosol. Nature *429*, 841–847.

Yeung, H.O., Kloppsteck, P., Niwa, H., Isaacson, R.L., Matthews, S., Zhang, X., and Freemont, P.S. (2008). Insights into adaptor binding to the AAA protein p97. Biochem. Soc. Trans. *36*, 62–67.